Calcium Carbonate Decomposition under External Pressure Pulsations

Patil, K., Jain, S., Gandi, R. K., Shankar, H. S.*,
Department of Chemical Engineering
Indian Institute of Technology Bombay, Powai, Mumbai-400076, India
E-mail: hss@che.iitb.ac.in, gandi@iitb.ac.in, kiranp@iitb.ac.in, swatijain@iitb.ac.in

Abstract

In this work effect of pulsating flow on thermal decomposition of a spherical pellet of calcium carbonate is presented. Here we use grain model and solve the unsteady state diffusion reaction equations under external pressure pulsations. The effects on temperature, conversion-time and radial profiles are predicted. It is shown that under pulsating pressure significant improvements in conversion time behaviour can be obtained for diffusion limited conditions. Experimental data are presented to validate the predictions and also pointer applications where such methods might be useful.
Key words: Calcium carbonate, Decomposition, Transport processes in Pulsating flow

1 Introduction

Calcination of limestone, high temperature reactions of cement kilns, smelting of ores, sulfur capture from gases, solid catalysed reactions, drying of grains and industrial products are very large scale examples where heat and mass transfer play crucial role. Limestone calcination technology engages rotary kiln (RK), fluidized beds (FB) and vertical shaft kilns (SK). RK and FB are common for very large scales a million ton/yr plus, while shaft kilns are used for small scales. Limestone decompositions are also carried out in very large quantities in decentralised very small scale may be 2-10 tons per batch using local ores and sea shells. At these scales extent of calcination is an important quality issue. In very large scales all such issues are factored into design by choosing the appropriate scales. In this light the technology of heat and mass transfer need fresh appraisal.

In the normal range of 700-1000°C, the calcination products are calcium oxide and carbondioxide. According to Satterfiled and Feaks (1959) and Ingraham and Marrier (1962) the reaction is controlled by chemical reaction. Narsimhan (1959) postulated that there is no internal temperature gradient and all the heat reaching decomposition plane is used up for the endothermic decomposition. Rao et al., (1989) considered a grain model , solved the unsteady diffusion reaction model for the grain wherein the temperature effects were described by the Prater relationship

$$T_0 - T = \frac{C_{A0} - C_{As}}{h_T/k_g \Delta H} + \frac{C_{As} - C_A}{k_e/D_e \Delta H} \tag{1}$$

where T_0 is bulk temperature, s refers to surface values and the terms in the right are the temperature drop in gas film and in the solid layer; and showed that the pellet conversion temperature-time data could be described adequately by the diffusion reaction model. Murthy (1994) also considered grain model and solved the diffusion reaction equations for simultaneous mass amd heat transfer, also

*Address all correspondence to this author

taking into account the effects of porosity, effective diffusivity and effective thermal conductivity changes in the pellet. The results revealed good agreement with conversion-time data and that the variation in k_e, D_e were not significant to affect the conversion-time predictions.

Introduction of presssure pulsation is an useful way of enhancing the rates of transport processes and has been studied earlier. Increase in rates of reduction of iron ore pellets by hydrogen was found by Ohmi and Usui (1976b) when pulsating conditions were applied. Hamer and Cormack (1978) investigated the utility of periodic external pressures for increasing rates of catalytic reactions in porous catalyst pellets. Sohn and Chaubal (1984) investigated the effects of cycling external pressure for gas solid reactions. Sohn and Aboukheshem (1992) conducted an experimental study on the reduction of nickel oxide by hydrogen. Fraenkel and Nogueira (1998) found enhanced rates of drying when a pulsating field was created by oscillating flow. Ballal (1995) developed a simple model to demonstrate the effect of pressure pulsations on mass transfer through pores. It was found that mass transfer rates can be enhanced when Peclet number and amplitude of pulsing are large.

Maithy(1997) conducted experiments to study the effects of pulsating external pressure at frequency upto 1.25 Hz and A = 0.125 for limestone decomposition in a bed of coal-limestone mixture; Results were promising. Dias et al(2004) conducted experiments on drying of soyabean at A=0.278 atm and frequency of 70 Hz, at 60°C and different moisture content of gas solid. It was found that under pulsating pressure, conversions-time behaviour showed significant improvement for NiO reduction while not effective for drying of soyabean.

In this work (Patil et al, 2004) we focus on the model of the process; compare predictions with experimental data and delineate applicability of the pulsating procedure.

2 Model

At high temperatures (about 900°C), calcium carbonate decomposes to give solid calcium oxide and carbon dioxide gas.

$$\begin{aligned} CaCO_3(s) &\rightarrow CaO(s) + CO_2(g) \quad \Delta H = 178kJ/mol \\ B(s) &\rightarrow C(s) + A(g) \end{aligned}$$

where A is CO_2, B is $CaCO_3$ and C is CaO. Following simplifying assumptions are made in the model:

1. The pellet is made up uniform spherical non-porous grains typically of 6 micron radius (r_g).
2. The grains are uniformly distributed over the pellet volume and the macroscopic structure is unaffected as the reaction progresses
3. There is no temperature graident and concentration gradient inside the grain.
4. The change in temperature and concentration have little effect on the activation energy, effective diffusivity, effective thermal conductivity, heat and mass transfer coefficients and heat of reaction.
5. Permeability of calcium carbonate and calcium oxide is high leading to negligible internal pressure gradient.
6. The pressure pulsations are represented as

$$P = P_0(1 + Asin(2\pi ft)) \tag{2}$$

Mass balance on gas A gives

$$\begin{aligned} \frac{\partial C_A}{\partial t} =& AD_e\{\frac{\partial^2 C_A}{\partial r^2} + p\frac{2}{r}\frac{\partial C_A}{\partial r}\}+ \\ & \frac{1}{p}\frac{dp}{dt}\{\frac{r}{3}\frac{\partial C_A}{\partial r} + C_A\} + r_A \end{aligned} \tag{3}$$

The energy balance equation for pellet is given as

$$\begin{aligned}\rho_p C_p \frac{\partial T}{\partial t} =& K_e\{\frac{\partial^2 T}{\partial r^2} + \frac{2}{r}\frac{\partial T}{\partial r}\} + \frac{C_{pa}}{RT_0}\frac{dp}{dt}\{T \\ &+ \frac{r}{3}\frac{\partial T}{\partial r}\} - (\Delta H) r_A\end{aligned} \tag{4}$$

The balance for solid calcium carbonate grain B gives

$$-\rho_B \frac{\partial r_g}{\partial t} = K_r\{1 - \frac{C_A}{C_E}\}^n \tag{5}$$

The rate of reaction r_A is given by

$$r_A = \frac{3(1-\epsilon_0) r_g^2 K_r\{1 - \frac{C_A}{C_E}\}^n}{r_{g_0}^3}\} \tag{6}$$

C_E is determined by equilibrium partial pressure of CO_2 givenn by Hill and Winter (1956) as

$$log_{10} p_E = -\frac{8792.3}{T} + 10.4022 \tag{7}$$

The initial and boundary conditions for the pellet are

$$C_A = C_{E0} \quad \forall r \text{ at t=0} \tag{8}$$

$$T = T_0 \quad \forall r \text{ at t=0} \tag{9}$$

$$r_g = r_{g_0} \quad \forall r \text{ at t=0} \tag{10}$$

$$\frac{\partial C_A}{\partial r}|_{r=0} = 0 \qquad \text{at t} \geq 0 \tag{11}$$

$$\frac{\partial T}{\partial r}|_{r=0} = 0 \qquad \text{at t} \geq 0 \tag{12}$$

$$-D_e \frac{\partial C_A}{\partial r}|_{r=r_0} = k_g(C_{As} - C_{A_0}) \text{ at t>0} \tag{13}$$

$$K_e \frac{\partial T}{\partial r}|_{r=r_0} = -h_T(T_s - T_0) \text{ at t>0} \tag{14}$$

The fractional conversion for the whole pellet at any time is given by

$$X = 1 - \frac{3}{r_{g_0}^3 r_0^3}\int_0^{r_0} r_g^3 r^2 dr \tag{15}$$

Molar density of calcium carbonate (29.3kmol/m^3) is almost half the molar density of calcium oxide (59.2kmol/m^3) and hence there will be an increase in porosity during the reaction. The equation governing porosity change inside the pellet is given by

$$(1-\epsilon) = (1-\epsilon_0)\{z + \frac{r_g^3}{r_{g_0}^3}(1-z)\} \tag{16}$$

The effective diffusivity is given by (Murthy, 1994)

$$D_e = \frac{D_A}{\epsilon_0^{1/3}\tau_0}\{1 - (1-\epsilon_0)[z + \frac{r_g^3}{r_{g_0}^3}(1-z)]\}^{4/3} \tag{17}$$

and the effective thermal conductivity is given by

$$\begin{aligned}K_e =& K_B(1-\epsilon_0)[(1 - \frac{K_C}{K_B})\frac{r_g^3}{r_{g_0}^3} + \frac{K_C}{K_B}] \\ &[z + \frac{r_g^3}{r_{g_0}^3}(1-z)]\end{aligned} \tag{18}$$

The equations are nondimensionalised as per representation given in nomenclature.

Non Dimensional Equations

$$D_e = D_I F_D(\psi) \tag{19}$$

$$K_e = K_I F_K(\psi) \tag{20}$$

where

$$D_I = \frac{D_A}{\epsilon_0^{1/3}\tau_0} \tag{21}$$

$$F_D(\psi) = \{1-(1-\epsilon_0)[z+\psi^3(1-z)]\}^{4/3} \tag{22}$$

$$F_K(\psi) = (1-\epsilon_0)[(1-\lambda)\psi^3+\lambda][z+\psi^3(1-z)] \tag{23}$$

The governing partial differential equations become as

$$\begin{aligned}\frac{\partial\eta}{\partial\theta} =& \frac{\tau_4 F_D(\psi)}{\tau_3}[\frac{\partial^2\eta}{\partial\xi^2}+\frac{2}{\xi}\frac{\partial\eta}{\partial\xi}]+\frac{\tau_4}{\tau_1}\frac{Acos(\frac{\tau_4\theta}{\tau_1})}{(1+Asin(\frac{\tau_4\theta}{\tau_1}))}* \\ & [\frac{(\eta\phi-1)}{\phi}+\frac{\xi}{3}\frac{\partial\eta}{\partial\xi}]-\frac{\tau_4}{\tau_2}\frac{\psi^2}{\phi^3}e^{\alpha(1-\frac{1}{\omega})}\frac{(\eta-\eta_E)^n}{(1-\phi\eta_E)^n}\end{aligned} \tag{24}$$

$$\begin{aligned}\frac{\partial\omega}{\partial\theta} =& F_K(\psi)[\frac{\partial^2\omega}{\partial\xi^2}+\frac{2}{x}\xi\frac{\partial\omega}{\partial\xi}]+\frac{\tau_4\kappa v_0}{\tau_1}Acos(\frac{\tau_4\theta}{\tau_1})* \\ & [\omega+\frac{\xi}{3}\frac{\partial\omega}{\partial\xi}]-\frac{\tau_4}{\tau_2}\frac{\beta\psi^2}{\phi^3}e^{\alpha(1-\frac{1}{\omega})}\frac{(\eta-\eta_E)^n}{(1-\phi\eta_E)^n}\end{aligned} \tag{25}$$

$$\frac{\partial\psi}{\partial\theta} = -\frac{\tau_4}{\tau_2}\frac{\gamma}{\phi^2}e^{\alpha(1-\frac{1}{\omega})}\frac{(\eta-\eta_E)^n}{(1-\phi\eta_E)} \tag{26}$$

The initial and boundary conditions transform into

$$\eta = 0 \quad at \quad \theta = 0 \quad for \quad all \quad \xi \tag{27}$$

$$\omega = 1 \quad at \quad \theta = 0 \quad for \quad all \quad \xi \tag{28}$$

$$\psi = 1 \quad at \quad \theta = 0 \quad for \quad all \quad \xi \tag{29}$$

$$\frac{\partial\eta}{\partial\xi} = 0 \text{at } \xi = 0, \theta = 0 \tag{30}$$

$$\frac{\partial\omega}{\partial\xi} = 0 \text{at } \xi = 0, \theta = 0 \tag{31}$$

$$\frac{\partial\eta}{\partial\xi} = \frac{Bi_M}{F_D(\psi)}(1-\eta_s) at \xi = 1, \theta > 0 \tag{32}$$

$$\frac{\partial\omega}{\partial\xi} = \frac{Bi_H}{F_K(\psi)}(1-\omega_s)\xi = 1, \theta > 0 \tag{33}$$

The equation for fractional conversion can be written as

$$X = 1 - 3\int_0^1 \psi^3\xi^2 d\xi \tag{34}$$

3 Results

The equations in Section 2 above describe the variation of temperature, concentration, grain radius in terms of position and time. The nondimensionalised equations of Section 2 present the same picture in a more useful way since the parameters that appear can be estimated and so the relative importance of the processes at work can be identified from the time constants. In the present case

pulsing time τ_1 ($\frac{1}{2\pi f}$ = 1.4s), reaction time τ_2 ($\frac{1}{k}$ = 5x10^{-3}s), mass diffusion time for CO_2 τ_3 ($\frac{r_0^2}{D_e}$ = 5.66s) and thermal diffusion time τ_4 ($\frac{r_0^2 \rho C_p}{k_e}$ = 256s for $CaCO_3$ or 0.36 for CO_2) indicate that diffusional availability of heat in the solid is the slowest process. Accordingly the non dimensional time(θ) is defined on the basis of thermal diffusion time. Note that pulsing time can also be given as τ_5 = r_0/v where v (= $\frac{-r}{p}\frac{dp}{dt}$) is the velocity in pore space.

The nondimensional equations are converted into ordinary differential equations using central finite difference technique. Crank Nicholson technique, which is average of both explicit and implicit methods is used to solve the resulting ordinary differential equations (Golub and Ortega, 1992). Stability of numerical procedure is asserted by appropriate choice of step size in time and space.

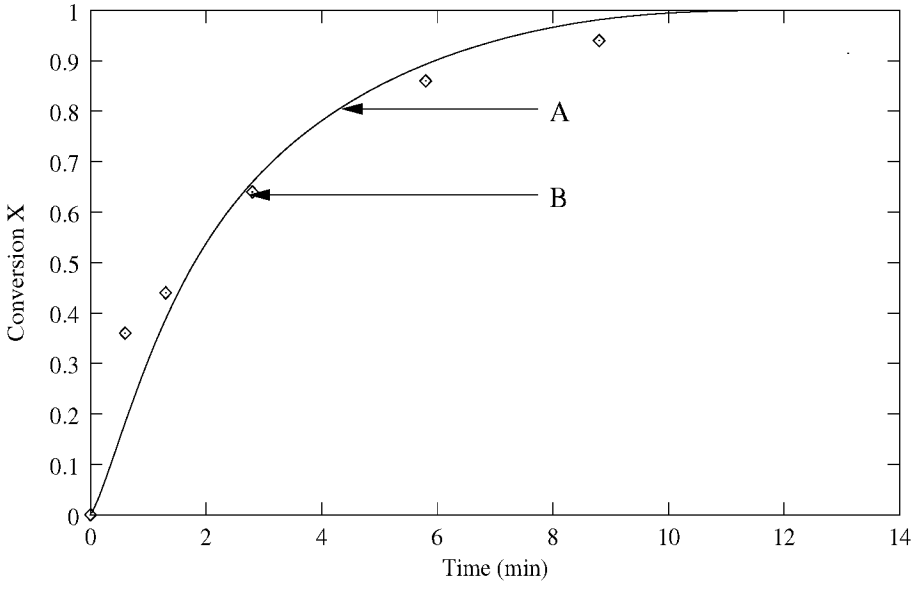

Figure 1: Conversion vs time profile for single pellet reduction of nickel oxide showing very good agreement between numerical result and experimental data, Curve A : Numerical, Curve B : Experimental (Sohn and Aboukheshem, 1992); Temperature of reaction = 653K, Amplitude of Pulsing (A) = 0.22, Frequency of pulsing (f) = 10Hz, Effective diffusivity (D_e) = 3.66x10$^{-5}m^2s^{-1}$, Reaction rate constant (k) = 1105x10$^{-6}m^3mol^{-1}s^{-1}$, Mole fraction of H_2 in bulk = 1.0

The numerical method used was verified by comparing the solution with analytical solution (Bailey and Ollis, 1986) for the case of unsteady heat transfer to solid spheres wherein excellent reproduction was obtained. The same numerical procedure was used to predict conversion time behaviour of nickel oxide reduction data of Sohn and Aboukheshem (1992) under pulsating flow. The prediction of instantaneous radial profile temperature and concentration are presented as time average over the pulsating time period τ_1. Figure 1 showing the good agreement between data and numerical predictions reveals that the numerical methods are satisfactory.

Figure 2 shows comparison between experimental data of Rao et al(1989) at 1150 K and predicted values of conversion-time relationship for calcium carbonate taking both material and

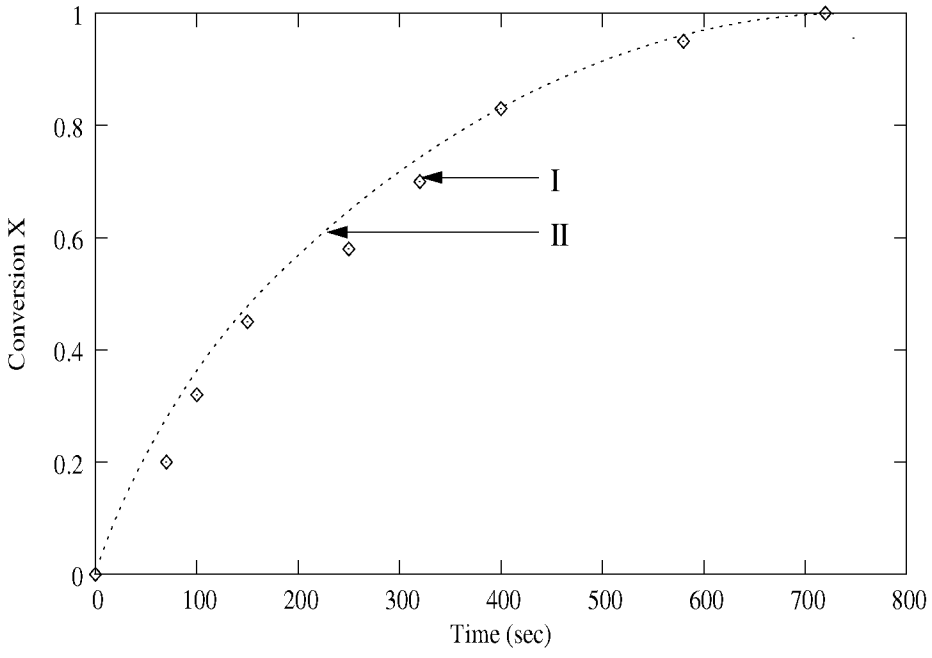

Figure 2: Conversion vs time profile for single pellet decomposition of $CaCO_3$ showing very good agreement between numerical result and experimental data, Curve I : Experimental (Rao et al., 1989), Curve II : Numerical; Pellet radius $r_p = 3.7\text{x}10^{-3}$m, Bulk temperature $T_0 = 1150$K, Grain radius $r_{g_0} = 5\text{x}10^{-6}$m, Diffusivity of CO_2 in $CaCO_3$ $D_a = 5.5\text{x}10^{-5}\text{m}^2/\text{s}$, Bulk concentration of CO_2 $C_{A_0} = 1.0\text{x}10^{-5}\text{kmol/m}^3$, Biot number for mass $B_{iM} = 3.5$, Biot number for heat $B_{iH} = 1.5$

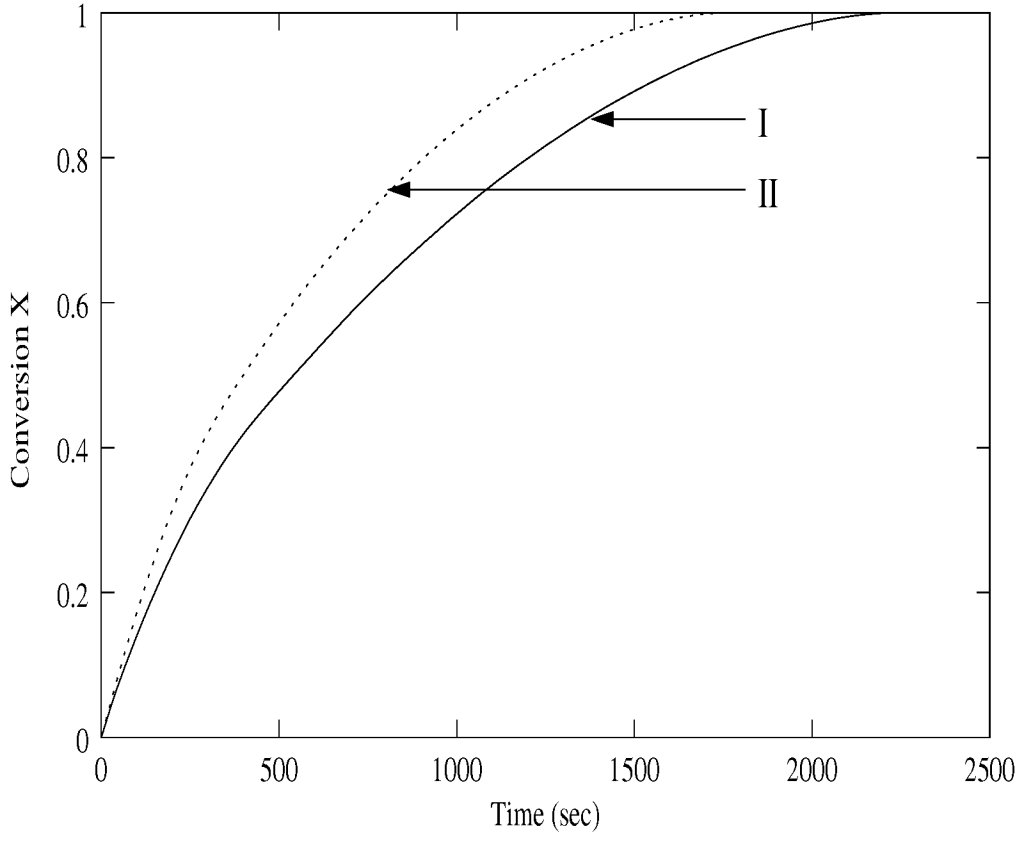

Figure 3: Single pellet prediction of conversion with time for grain model of solid $CaCO_3$ decomposition, Curve I (using Material and Energy balance equations) : Amplitude A = 0, Curve II (using only Material balance equations) : Amplitude A = 0.25, Frequency of pulsation f = 0.16Hz; Pellet radius $r_p = 6.0 \text{x} 10^{-3}$m, Bulk temperature $T_0 = 1113$K, Grain radius $r_{g_0} = 3 \text{x} 10^{-6}$m, Diffusivity of CO_2 in $CaCO_3$ $D_a = 4 \text{x} 10^{-5} \text{m}^2/\text{s}$, Bulk concentration of CO_2 $C_{A_0} = 1 \text{x} 10^{-5} \text{kmol/m}^3$, Biot number for mass $B_{iM} = 0.75$, Biot number for heat $B_{iH} = 2.0$

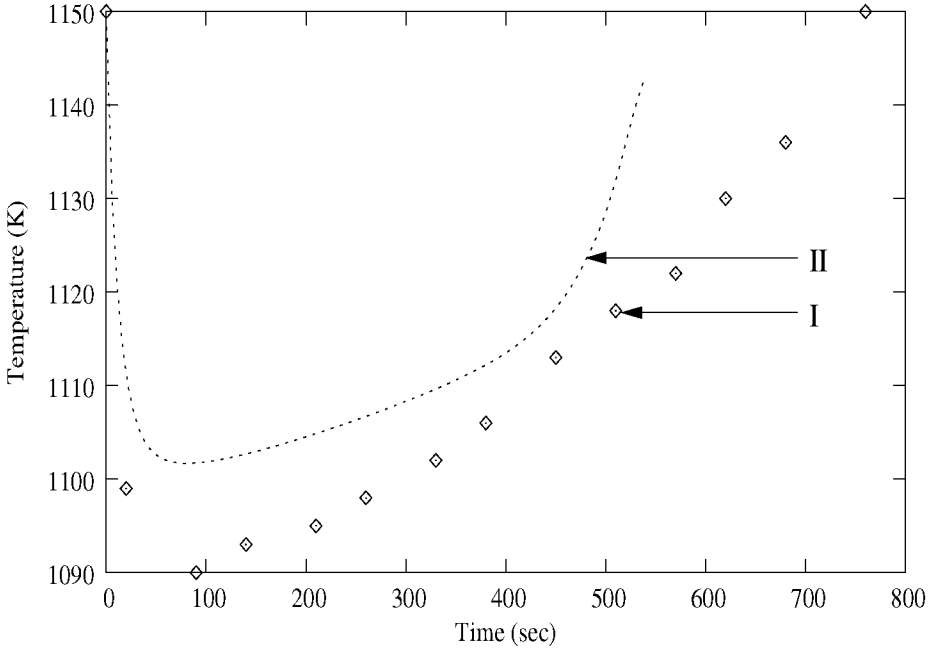

Figure 4: Temperature vs time profile for single pellet decomposition of $CaCO_3$ showing agreement between numerical result and experimental data, Curve I : Experimental (Rao et al., 1989), Curve II : Numerical; Pellet radius $r_p = 3.7\text{x}10^{-3}$m, Bulk temperature $T_0 = 1150$K, Grain radius $r_{g_0} = 5\text{x}10^{-6}$m, Diffusivity of CO_2 in $CaCO_3$ $D_a = 2.5\text{x}10^{-5}\text{m}^2/\text{s}$, Bulk concentration of CO_2 $C_{A_0} = 1.0\text{x}10^{-5}\text{kmol/m}^3$, Biot number for mass $B_{iM} = 3.5$, Biot number for heat $B_{iH} = 1.5$. The discrepancy between model prediction and data is due to inadequate information on system parameters.

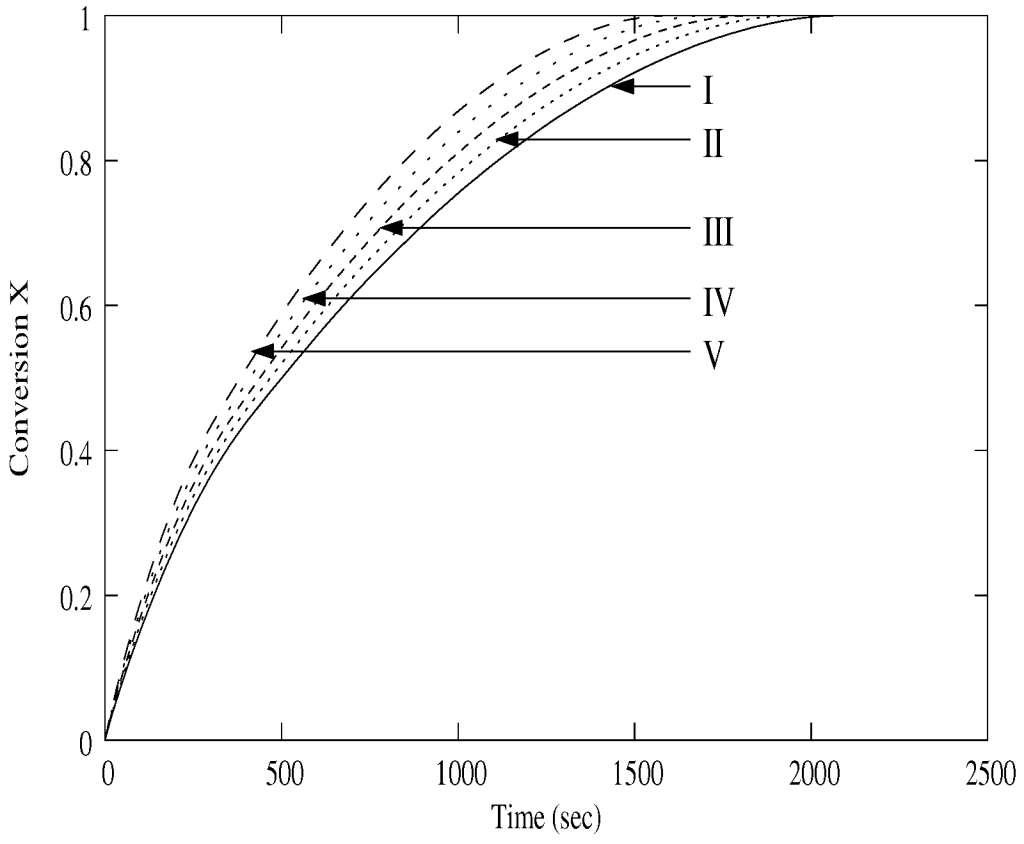

Figure 5: Effect of frequency for Single pellet prediction of conversion vs time for grain model of solid $CaCO_3$ decomposition showing higher conversion as frequency of pulsation is increased, Curve I : Frequency f = 0.08Hz, Curve II : Frequency f = 0.16Hz, Curve III : Frequency f = 0.32Hz, Curve IV : Frequency f = 0.64Hz, Curve V : Frequency f = 1.28Hz; Amplitude of pulsation A = 0.25, Pellet radius $r_p = 6.0\text{x}10^{-3}$m, Bulk temperature $T_0 = 1113$K, Grain radius $r_{g_0} = 6\text{x}10^{-6}$m, Diffusivity of CO_2 in $CaCO_3$ $D_a = 4\text{x}10^{-5}\text{m}^2/\text{s}$, Bulk concentration of CO_2 $C_{A_0} = 1\text{x}10^{-5}\text{kmol}/\text{m}^3$, Biot number for mass $B_{iM} = 2.0$, Biot number for heat $B_{iH} = 0.75$.

energy balance equations into account. Prediction of the same data using mass balance alone (not shown) was poor. Figure 3 illustrates differences in the predictions based on mass and energy balance (curve I) and mass balance alone (curve II); the lower conversion attained in curve I indicates that retention times depend upon heat energy availability for the endothermic reaction. Figure 4 shows comparison between experimental and predicted surface temperature-time profile; Results shows that temperature variation is small and is well packed up by model. The minor disagreement seen is due to inadequate knowledge of the parameter values of the data. Figure 5 shows the conversion-time predictions for different frequency. The time for complete conversion 2254 s for A=0 (=8.79 τ_4) to 1500 s at A = 0.25 and f=1.28 Hz is indicated . In view of the more favourable concentration of reactant in contact with pellet the observed decrease in the time required for reaction. Figures 6 and 7 show radial profiles of concentrations and temperature. These results reveal that A and f determnine bulk flow velocity (v = $\frac{-r}{p}\frac{dp}{dt}$) in pore space, hence the observed decrease in time required for reaction. Figure 8 shows radial temperature and Figure 9 shows concentration profiles for two situations viz I:solution of the system equation, II:solution of the system equations by deleting the pulsating term and adjusting the thermal conductivity (thermal diffusion coefficient) to fit the predictions of curve I. The approximate description obtained in II shows that for the situations up to f $\leq$ 0.16 and A $\leq$ 0.5 or equivalently a bulk flow velocity of 3.0 x 10^{-3}m/s, the approximation is satisfactory and the effect of pulsating term can be approximated by an equivalent apparent diffusion coeffcient. The results of Figures 6-9 show that the radial temperature variation is small $\simeq \Delta\omega$ 0.001-0.002 (ΔT$\simeq$1°C) indicating that the pellet is essentially at T_s.

Maity (1997) conducted experiments to study the effect of pulsating flow on limestone decomposition. He prepared pellets of $CaCO_3$ and coal mixture and combusted them in a packed bed with pulsating pressure across the bed. The heat for decomposition was provided by the burning coal. Temperature-time data was recorded at four different positions in the bed and extent of decomposition found at those positions by sampling. The values of the extent of dissociation for nonpulsating conditions ranged between 80-87% for those locations where the temperatures are higher than about 1000°C. The average ranged between 81-83%. On the other hand the average conversion values were almost always higher than 90% when the pressure was pulsated. Thus pressure pulsation increased the overall extent of reaction.

The experimental parameters of Maithy (1997) were applied to the present model and predictions of conversion vs time profiles were obtained. Table 2 gives the experimental and model results for decomposition under nonpulsating and pulsating conditions. Average time, temperature and conversion at the 4 positions where temperature and conversion was measured is taken and shown in Table 2. The temperature of reaction is taken equal to the average temperature measured for each run. Predicted conversion time profiles for single pellet case were found for different runs. Time required to achieve the experimental average conversion is also predicted and shown in Table 3. The results show consistency of model with experimental data. However experimental time (for X = X_{av}) higher than predicted time (for X = X_{av}) is indicated in Table 2; this implies that pellets are not at the average temperature indicated.

Table 3 summarizes the time constants for the processes taking place for three reactions : a) reduction of metal oxide data of Sohn and Aboukheshem (1992), b) Calcium carbonate decomposition, c)soya bean drying of Dias et al (2004). Experimental data of Sohn and Aboukheshem (1992) for metal oxide shows significant conversion-time improvement due to pulsating external pressure; while data of Dias et al (2004) for soya bean drying at 70 Hz shows no effect due to pulsating pressure. The above feature of the data can be explained from the time constants shown in Table 3.

In the case of Nickel oxide with highly non linear kinetics the process is controlled by diffusional resistance (τ_3, τ_4) and the small ratio τ_1/τ_3 of 0.001 brings about significant decrease in the overall resistance. In the case of soyabean drying, the process is controlled by bound moisture with τ_2 (= large) and so there is no effect; this feature perhaps arises from vapour pressure of condensed water in the capillaries being very low as per Kelvin equation. In the case of calcium carbonate decomposition which is controlled by thermal diffusion τ_4 (= 256 s) the ratio τ_1/τ_4 is 0.002, hence the observed similar results as that of NiO.

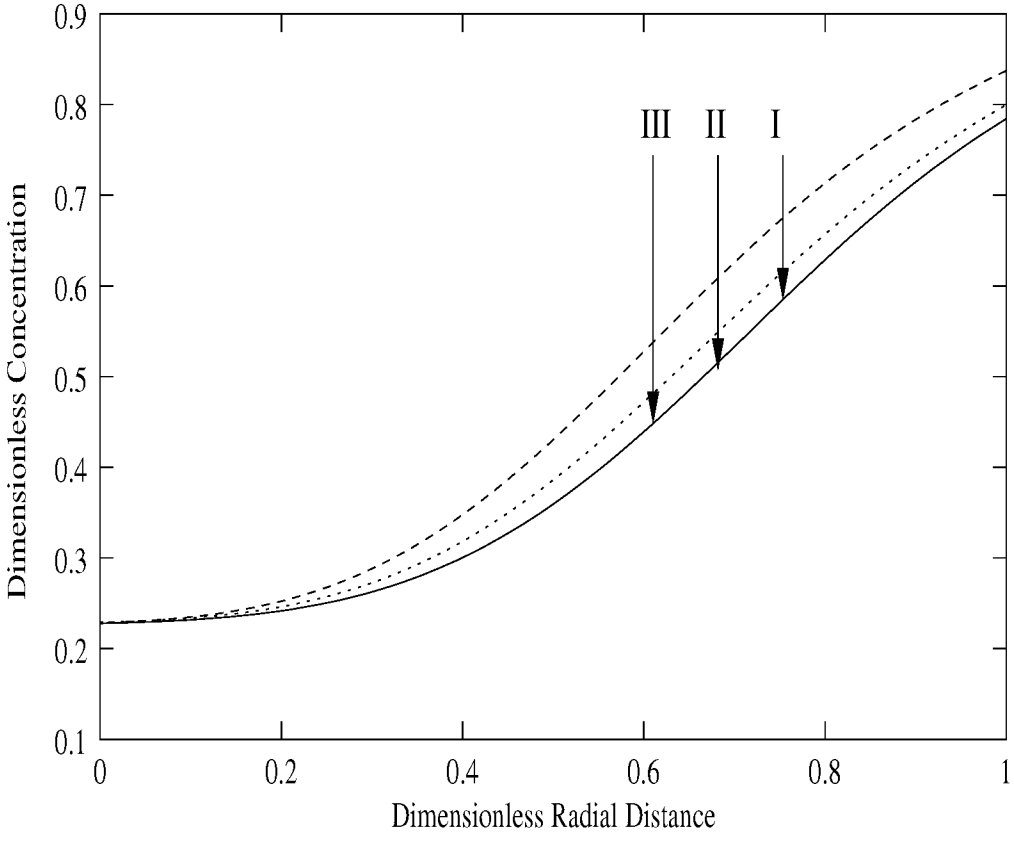

Figure 6: Single pellet prediction of dimensionless CO_2 concentration vs dimensionless radial for grain model of solid $CaCO_3$ decomposition for different amplitudes of pulsation 1556 sec after the start of reaction showing effect of pulsing amplitude on CO_2 concentration, Curve I : Amplitude A = 0, Curve II : Amplitude A = 0.25, Curve III : Amplitude A = 0.5; frequency of pulsation f = 0.16Hz, Pellet radius $r_p = 6.0 \times 10^{-3}$m, Bulk temperature $T_0 = 1113$K, Grain radius $r_{g_0} = 3 \times 10^{-6}$m, Diffusivity of CO_2 in $CaCO_3$ $D_a = 4 \times 10^{-5}$m^2/s, Bulk concentration of CO_2 $C_{A_0} = 1 \times 10^{-5}$kmol/m^3, Biot number for mass $B_{iM} = 0.75$, Biot number for heat $B_{iH} = 2$. Higher amplitude of pulsation enhances the diffusion of CO_2.

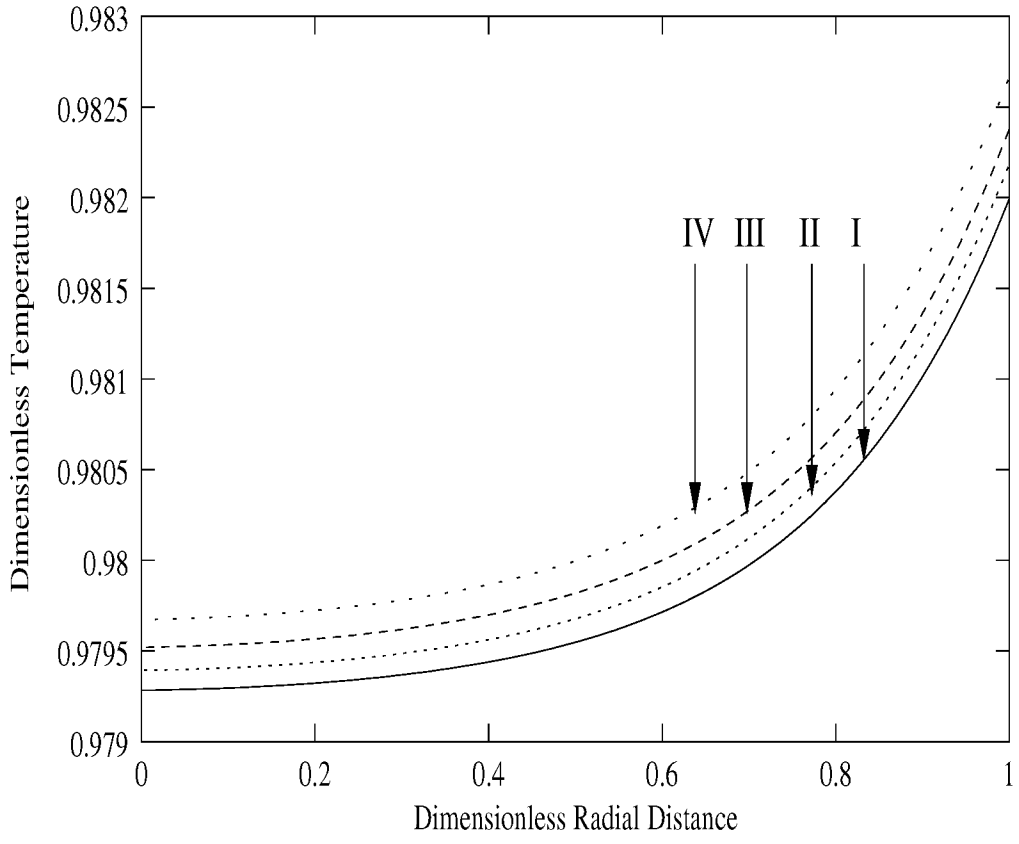

Figure 7: Single pellet prediction of dimensionless temperature vs dimensionless radial position of pellet for grain model of solid $CaCO_3$ decomposition for different frequencies of pulsation 286s after the start of reaction showing effect of pulsing frequency on temperature of pellet, Curve I : frequency f = 0.16Hz, Curve II : frequency f = 0.32Hz, Curve III : frequency f = 0.64Hz, Curve IV : frequency f = 1.28Hz, Amplitude of pulsation A = 0.25, Pellet radius $r_p = 6.0 \times 10^{-3}$m, Bulk temperature $T_0 = 1113$K, Grain radius $r_{g_0} = 3 \times 10^{-6}$m, Diffusivity of CO_2 in $CaCO_3$ $D_a = 4 \times 10^{-5}$m^2/s, Bulk concentration of CO_2 $C_{A_0} = 1 \times 10^{-5}$kmol/m^3, Biot number for mass $B_{iM} = 0.75$, Biot number for heat $B_{iH} = 2$. Higher frequency of pulsation enhances the diffusion of heat.

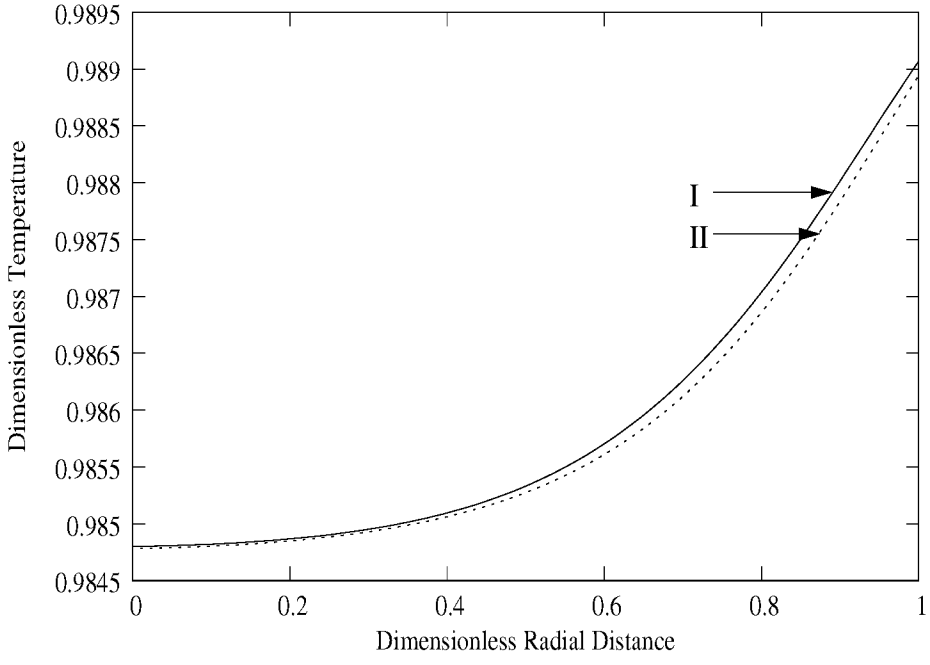

Figure 8: Radial temperature variation showing numerical solution curve I and approximate numerical solution curve II for single pellet decomposition of calcium carbonate modelling of pulsating pressure showing dimensionless temperature versus dimensionless radial distance, Curve I (pulsating pressure) : Amplitude A = 0.5, Frequency of Pulsation = 0.16Hz Thermal Conductivity K_B = 1.4J/mKs, Curve II (approximate solution by deleting pulsating pressure term by setting A=0 and adjusting thermal conductivity) : Amplitude A = 0.0, Thermal Conductivity K_B=1.5J/mKs; Pellet radius $r_p = 6.0\text{x}10^{-3}$m, Bulk temperature T_0 = 1113K, Grain radius $r_{g_0} = 6\text{x}10^{-6}$m, Diffusivity of CO_2 in $CaCO_3$ $D_a = 4\text{x}10^{-5}\text{m}^2/\text{s}$, Bulk concentration of CO_2 $C_{A_0} = 1\text{x}10^{-5}\text{kmol/m}^3$, Biot number for mass B_{iM} = 2.0, Biot number for heat B_{iH} = 0.75

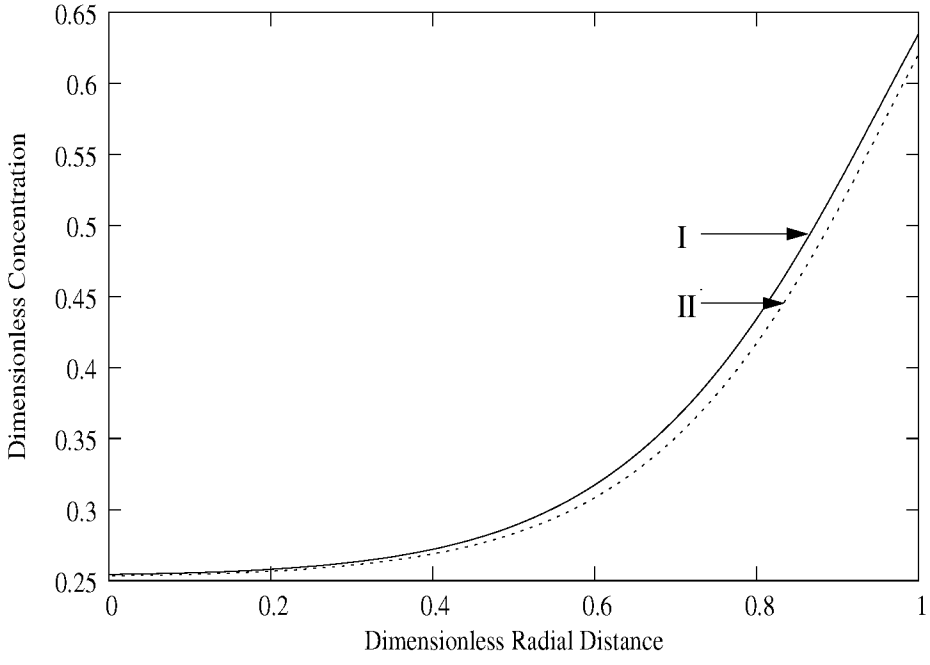

Figure 9: Radial concentration profile showing numerical solution curve I and approximate solution curve II for single pellet decomposition of calcium carbonate modelling of pulsating pressure showing dimensionless concentration versus dimensionless radial distance, Curve I : (pulsating pressure) Amplitude A = 0.5, Frequency of Pulsation = 0.16Hz Thermal Conductivity K $_B$ = 1.4J/mKs, Curve II : (approximate solution by deleting pulsating pressure term by setting A=0 and adjusting thermal conductivity) Amplitude A = 0.0, Thermal Conductivity K_B=1.5J/mKs; Pellet radius r_p = 6.0x10^{-3}m, Bulk temperature T_0 = 1113K, Grain radius r_{g_0} = 6x10^{-6}m, Diffusivity of CO_2 in $CaCO_3$ D_a = 4x10^{-5}m^2/s, Bulk concentration of CO_2 C_{A_0} = 1x10^{-5}kmol/m^3, Biot number for mass B_{iM} = 2.0, Biot number for heat B_{iH} = 0.75

Table 1: Values of different parameters used for decomposition of $CaCO_3$

ρ_B	29.3	kmol/m^3
ρ_C	59.2	kmol/m^3
n	2	-
C_p	1.268x10^5	J/kmolK
D_A	2x10^{-5}	^{2}/s
ΔH	1.78x10^8	J/kmol
E	1.75x10^5	J/mol
K_B	1.4	J/mKs
K_C	7	J/mKs
K_{r0}	2.45x10^{-5}	kmol/m^{2}s
R_g	8.314	J/molK
C_{A0}	1x10^-5	kmol/m^3
ϵ_0	0.63	-
r_{g_0}	3x10^{-6}	m
r_0	5.975x10^{-3}	m
T_0	1113	K
τ_0	2	-
f	$1/2\pi$	Hz
h_T	58.5	J/m^{2}Ks
k_g	5x10^{-3}	m/s
$\Delta\xi$	-0.1	-
$\Delta\theta$	0.000001	-
C_{E0}	4.5x10^{-3}	kmol/m^3
B_{iM}	1.5	-
B_{iH}	0.25	-
κ	0.253	-
α	18.99	-
v_0	3.69x10^{-4}	-
β	1.97x10^{-4}	-
τ_1	1	s
τ_2	5.04x10^{-3}	s
τ_3	5.66	s
τ_4	256.05	s

Table 2: Comparison of packed bed experimental data of Maity (1997) and predictions of single pellet model of Patil (2004)

No	A	f	T_{avg}	X_{avg}	$Time_{avg}$	$Time_{predicted}$	$Time_{predicted}$
		Hz	°C	% (experimental)	s (experimental)	s (for X=100%)	s (for $X=X_{avg}$
1	0	-	900	79	129	560	95
2	0	-	1057	81	115	203	107
3	0	-	1121	81	133	199	100
4	0	-	1178	83	140	140	73
5	0	-	1186	83	137	131	65
6	0	-	1321	81	116	110	53
7	0.125	0.3	1146	92.5	160	141	93
8	0.125	0.33	1089	90	160	169	106
9	0.125	0.33	1140	92.5	223	141	94
10	0.125	0.33	1146	92.5	160	141	93
11	0.125	0.33	1252	83	112	114	56
12	0.125	0.75	1256	95	115	253	191
13	0.125	1.25	1292	94.5	111	190	138
14	0.125	0.33	1302	94	164	106	68
15	0.125	0.75	1345	96.3	119	162	123

Table 3: Time constants for some systems where τ_1 or τ_5 :pulsing time, τ_2:reaction time, τ_3:mass diffusion time, τ_4:thermal diffusion time. Diffusion times τ_3 refer to H_2/ H_2O mixture in NiO; CO_2 in $CaCO_3$ decomposition and water vapour for soya drying.

system	r_0	T	τ_1	τ_2	τ_3	τ_4	τ_5	source
	m	K	s	s	s	s	s	
NiO	0.01	573	0.03	0.385	33	10	0.04	Gandi (2004)
$CaCO_3$	0.006	1150	0.55	0.005	5.66	256	4	Patil (2004)
soyabean	0.01	333	0.002	$4x10^7$	10	160	0.008	Gandi (2004)

4 Conclusion

The work presented leads to following conclusions:

1. Calcium carbonate decomposition, temperature gradient in the pellet is small and that heat supply is the rate controlling step.
2. The effect of pulsating convective flow on temperature and concentration profile can be described approximately for small velocities v < 3mm/s by diffusion-reaction model with a higher value diffusion coefficient and without the pulsating convection term.
3. Pulsating pressure is useful if the diffusion time is a significant component of the overall reaction time.

Nomenclature

A	Dimensionless amplitude of pressure cycling
B_{iH}	Biot number for heat $\frac{h_T r_0}{K_I}$
B_{iM}	Biot number for mass $\frac{k_g r_0}{D_I}$
C_A	Concentration of reactant gas A $(kmol/m^3)$
C_{A0}	Concentration of reactant gas A initially $(kmol/m^3)$
C_{As}	Concentration of reactant gas A at surface $(kmol/m^3)$
C_E	Concentration of CO_2 in equilibrium with solid at any time and radial position$(kmol/m^3)$
C_{E0}	Concentration of CO_2 in equilibrium with solid at any radial position initially$(kmol/m^3)$
C_p	Molar specific heat of ($CaCO_3$) $(kmol/m^3)$
C_{pa}	Molar specific heat of air $(kmol/m^3)$
D_A	Bulk diffusivity (m^2/s)
D_e	Effective diffusivity (m^2/s)
D_I	Initial diffusivity (m^2/s)
f	Frequency of pulsing (Hz)
h_T	Total heat transfer coefficient (J/m^2Ks)
k_g	Mass transfer coefficient (m/s)
K_B	Thermal conductivity of $CaCO_3$ (J/mKs)
K_C	Thermal conductivity of CaO (J/mKs)
K_e	Effective thermal conductivity (J/mKs)
K_I	Initial thermal conductivity of $CaCO_3$ (J/mKs)
K_r	Reaction rate constant $(kmol/m^2s)$
n	Order of reaction
p	Total pressure (N/m^2)
p_E	Equilibrium partial pressure of $CO_2(N/m^2)$
r	Radial position at any given time (m)
r_0	Initial radius of pellet (m)
r_g	Average radius of grains (m)
r_{g0}	Initial average radius of grains (m)
t	Time (s)
T	Absolute temperature (K)
T_0	Bulk gas temperature (K)
T_s	Temperature at pellet surface (K)
v	velocity (m/s)
v_0	$\frac{p_0}{\rho_p R T_0}$
X	Conversion
z	Ratio of molar density of $CaCO_3$ to molar density of CaO
α	$\frac{E}{RT}$
ϕ	1-$\frac{C_{A0}}{C_{E0}}$
ΔH	Heat of reaction $(J/kmol)$
Δr	Step size in radial position (m)
ϵ_0	Initial porosity of pellet
ϵ	Porosity of pellet
η	Dimensionless concentration of CO_2 $\frac{1}{\phi}$(1-$\frac{C_A}{C_{E0}}$)
η_E	Dimensionless equilibrium gas concentration of CO_2 $\frac{1}{\phi}$(1-$\frac{C_E}{C_{E0}}$)
η_s	Dimensionless equilibrium concentration of CO_2 at surface of pellet
θ	Dimensionless time $\frac{t}{\tau_4}$
ξ	Dimensionless radial distance $\frac{r}{r_0}$
ρ	Molar density $(kmol/m^3)$
ρ_B	Molar density of $CaCO_3$ $(kmol/m^3)$
ρ_C	Molar density of CaO $(kmol/m^3)$

ρ_p Molar density of pellet $(kmol/m^3)$
τ_0 Initial tortuosity factor
τ_1 Pulsing time $\frac{1}{2\pi f}$ (s)
τ_2 Reaction time $\frac{C_{E0} r_{g0}}{3(1-\epsilon_0) K_{r0}}$ (s)
τ_3 Mass Diffusion time $\frac{r_0^2}{D_I}$ (s)
τ_4 Thermal diffusion time $\frac{\rho_p C_p r_0^2}{K_I}$ (s)
τ_5 Pulsing time (r_0/v) (s)
ψ Dimensionless radius of grain $\frac{r_g}{r_{g0}}$
ω Dimensionless temperature $\frac{T}{T_0}$
ω_s Dimensionless temperature at surface of pellet
γ $\frac{C_{E0}}{3(1-\epsilon_0)\rho_B}$
κ $\frac{C_{pa}}{C_p}$
λ $\frac{K_C}{K_B}$
β $\frac{\Delta H C_{E0}}{\rho_p C_p T_0}$

References

Ballal, N. B., 1995, Mass Transfer in Porous Solids Under Pulsating Pressure Conditions, *ISIJ International*, **258**, pp 446-448.

Bailey, J. E. and Ollis, D. F., 1986, Biochemical Engineering Fundamentals, McGrawHill, NewYork.

Dias, S.R.S., Futata, F.P.L., Carvalho, J.A., Couto, H.S. and Feireira, M.A., 2004, Investigation of food drying with pulsating flow, *International Commn Heat and Mass Transfer* , **31**, pp 387-395.

Frankel, S. L. and Nogueria, L. A. H., 1998, Heat Transfer Coefficients for Drying in Pulsating FLow, *International Commn Heat and Mass Transfer*, **25**, pp 471-480.

Gandi, R.K., Studies in Calcium carbonate decomposition under pulsating external pressure, M.Tech Thesis, Department of Chemical Engineering, IIT Bombay, July 2004.

Golub, G. H. and Ortega, J. M., 1992, Scientific Computing and Differential Equations.

Hamer, W. J. and Cormack, E. D., 1978, Influence of Oscillating External Pressure on Gas Phase Reactions in Porous Catalysts, *Chemical Engineering Science*, **33**, pp 935-944.

Hill, K. J. and Winter, E. R. S., 1956, Thermal Dissociation Pressure of Calcium Carbonate, *J. phys. Chem.*, **60**, pp 1361-1362.

Ingraham, T. R. and Marrier, P., 1963, Chemical Kinetics on the Thermal Decomposition of Calcium Carbonate, *Canadian Journal of Chemical Engineering*, **41**, pp 170-173.

Maithy, S. K., 1997, Effect of pressure pulsation on gas solid reaction in packed beds, *M.Tech. Thesis, Department of Metallurgical Engineering and Material Sciences, Indian Institute of Technology, Bombay*

Murthy, M. S., Harish, B. R., Rajanandam, K. S. and Ajoy Pavan Kumar, K. Y., 1994, Investigation on the Kinetics of Thermal Decomposition of Calcium Carbonate, *Chemical Engineering Science*, **49**, pp 2198-2204.

Narsimhan, G., 1961, Thermal Decomposition of Calcium Carbonate, *Chemical Engineering Science*, **16**, pp 7-20.

Ohmi, M. and Usui, T., 1976b, Therotical Investigation of Reaction Kinetics in the Reduction of Single Hematite Pellet Under Flow of Hydrogen, *Transcations ISIJ*, **16**, pp 85-91.

Patil, K., Studies in Calcium carbonate decomposition under pulsating external pressure, Dual Degree M.Tech thesis, Department of Chemical Engineering, IIT Bombay, July 2004.

Rajeswara Rao, T., Gunn, D. J. and Bowen, J. H., 1989, Kinetics of Calcium Carbonate Decomposition, *Chem Engg Res Des*, **67**, pp 38-47.

Satterfield, C. N. and Feakes, F., 1959, Kinetics of Thermal Decomposition of Calcium Carbonate, *A.I.Ch.E. J.*, **5**, pp 115-122.

Sohn, H. Y. and Aboukheshem, M. B., 1992, Gas-Solid Reaction-Rate Enhancement by Pressure Cycling, *Metalurgical Transactions B*, **23B**, pp 285-294.

Sohn, H. Y. and Chaubal, P. C., 1984, Rate Enhancement of the Gaseous Reduction of Iron Oxide Pellets by Pressure Cycling, *ISIJ* , **24**, pp 387-395.